JACS
JOURNAL OF THE AMERICAN CHEMICAL SOCIETY
Communication
pubs.acs.org/JACS

Photoconversion Bonding Mechanism in Ruthenium Sulfur Dioxide Linkage Photoisomers Revealed by in Situ Diffraction

Sven O. Sylvester,[†] Jacqueline M. Cole,*[,†,‡,§] and Paul G. Waddell[†,‡]

[†]Cavendish Laboratory, University of Cambridge, J. J. Thomson Avenue, Cambridge CB3 0HE, U.K.
Departments of [‡]Chemistry and [§]Physics, University of New Brunswick, P.O. Box 4400, Fredericton E3B 5A3, Canada

Supporting Information

ABSTRACT: Three new ruthenium−sulfur dioxide linkage photoisomeric complexes in the $[Ru(NH_3)_4(SO_2)X]Cl_2{\cdot}H_2O$ family (**X** = pyridine (**1**); 3-chloropyridine (**2**); 4-chloropyridine (**3**)) have been developed in order to examine the effects of the *trans*-ligand on the nature of the photo-induced SO_2 coordination to the ruthenium ion. Solid-state metastable η^1-O-bound (MS1) and η^2-side S,O-bound (MS2) photoisomers are crystallographically resolved by probing a light-induced crystal with in situ diffraction. This so-called photocrystallography reveals the highest known photoconversion fraction of 58(3)% (in **1**) for any solid-state SO_2 linkage photoisomer. The decay of this MS1 into the MS2 state was modeled via first-order kinetics with a non-zero asymptote. Furthermore, the MS2 decay kinetics of the three compounds were examined according to their systematically varying *trans*-ligand **X**; this offers the first experimental evidence that the MS2 state is primarily stabilized by donation from the $S{-}O_{bound}$ electrons into the Ru dσ-orbital rather than π-backbonding as previously envisaged. This has important consequences for the optoelectronic application of these materials since this establishes, for the first time, a design protocol that will enable one to control their photoconversion levels.

Photoisomerizable materials have potential applications in optoelectronic and photonic device technology, including optical switches and data storage.[1−6] Such compounds have optically accessible energy levels that are metastable and can act as binary switches: where the ground state isomer signifies "0" and the metastable state isomer signifies "1". Photoisomers with 3-D sensitive photorefractive properties also offer the option of 3-D data recording. As such binary data could be encoded according to the nature of the isomer, resulting in much larger density than current optical data storage methods.[5] Understanding the structural origins of the photophysical properties that govern photoisomerism is essential for optical data storage materials. Over the past decade, advances in in situ X-ray diffraction have enabled structural perturbations resulting from photoisomerization to be determined with sub-Ångstrom resolution.[7] This has afforded a direct relationship between the photoexcited molecular structure and the corresponding optical properties of a material.[8] However, for photoisomerizable crystals to be useful in such devices, controlled photoconversion is necessary and the thermal stability of the metastable photoinduced states would need to approach room temperature.[4]

One example of photoisomerizable crystals is the $[Ru(NH_3)_4(SO_2)X]Y$ family of complexes, where SO_2 is a photoactive linkage isomer that exists in the η^1-S-bound geometry for the ground state (GS), **X** is the ligand *trans* to SO_2 in the axial position, and **Y** is the counterion.[8−12] Two distinct photoexcited metastable states have been resolved crystallographically for this family: the η^1-O-bound (MS1) state and the more thermally stable η^2-side-S,O-bound (MS2) state (Figure 1). The MS1 state has been previously resolved

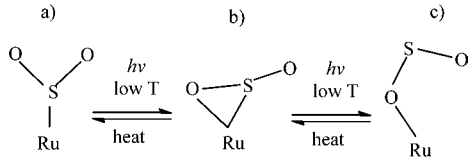

Figure 1. A schematic of the crystallographically resolved SO_2 geometries: (a) the η^1-S-bound (GS) geometry, (b) η^2-S,O-bound (MS2) geometry, (c) η^1-O-bound (MS1) geometry.

crystallographically in two compounds: first, the $[Ru(NH_3)_4(SO_2)(H_2O)]Tos_2$ complex where MS1 was captured at 13 K with an occupation of 34%, and was found to thermally decay between 13 and 100 K;[6] second, the $[Ru(NH_3)_4(SO_2)(H_2O)](\pm)$-camphorsulfonate complex with an MS1 population of 13%.[12] In this compound, the MS1 state decayed into the MS2 state at 120 K with a half-life of 3.4(8) h. However, owing to the low MS1 population, the precise kinetic nature of the decay could not be determined definitively. In both of these cases, the MS1, MS2, and GS geometries were shown to coexist.

The MS2 geometry has been examined in more detail, having been crystallographically resolved in six different compounds at 90−100 K.[8−11] The MS2 state occurs with 10−37% photoconversion with the remainder of the structure in the GS geometry. The decay kinetics of the MS2 state have been examined briefly using FTIR spectroscopy by Kovalevsky et al.[10,11] and it is thought that this state decays into the GS via first-order kinetics, and that its thermal stability is proportional to the Lewis basicity of the *trans*-ligand. Theoretical calculations have also been conducted on these compounds to examine the MS2 bonding geometry.[8,10,11] The MS2 bonding mode can be

Received: April 24, 2012
Published: June 29, 2012

   dx.doi.org/10.1021/ja303943q | J. Am. Chem. Soc. 2012, 134, 11860−11863

described as an analogue of the Dewar-Chat-Duncanson model for η^2-olefin bonding.[13] In this model, the S−O_{bound} π-electrons are donated into the empty Ru dσ-orbital, forming the primary σ-bond and this bond is then stabilized by backbonding from the Ru dπ-orbital to the ligand π^* antibonding orbitals of the S and O. Geometric manifestations of this can be seen by an extension of the S−O_{bound} bond, as the strength of the bond decreases with increased donation from the π-orbital into the Ru dσ-orbital. However, to date, it has not been determined experimentally whether the σ-donation into the empty Ru dσ-orbital or π-backbonding from the occupied dπ-orbital is the dominant force determining the stability of this state.

This communication reports three new *trans*-[Ru-$(NH_3)_4(SO_2)$**X**]$Cl_2{\cdot}H_2O$ complexes where **X** is pyridine (**1**), 3-chloropyridine (**2**), and 4-chloropyridine (**3**); this series permits a direct relationship to be made between the *trans*-ligand and the nature of the SO_2 photoisomerization. We find that the MS2 state can be crystallographically resolved for all three compounds with a maximum occupational fraction of 58(3)%, 10.4(1)%, and 18.2(7)% for **1**−**3** respectively. **1** also reveals a large occupation, 44.7(5)%, of the MS1 state; in **2**, there is no evidence of the MS1 state, while in **3** there is a small amount of electron density around the MS1 S atom, although this is too small to model. The decay kinetics of both the MS1 and MS2 states in **1** are examined at 120−140 and 200 K, respectively. We discover that MS1 decays exclusively into the MS2 state via first-order kinetics with a non-zero asymptote at 120 and 130 K before complete decay into the MS2 geometry at 140 K. The MS2 state decays via first-order kinetics into the GS and the MS2 geometry is primarily stabilized by donation from the S−O_{bound} π-electrons into the Ru dσ-orbital.

Photocrystallographic experiments on **1**−**3** were performed according to literature methods.[6,7] The crystals were mounted on a Rigaku Saturn 724+ CCD diffractometer equipped with a molybdenum X-ray source ($\lambda_{Mo,K\alpha}$ = 0.71073 Å) and accompanying SHINE optics. An Oxford Cryosystems CryostreamPlus open-flow nitrogen cooling device was used to cool the sample to 100 K and a full structure determination was performed; the experiment was conducted in complete darkness to prevent any background photoexcitation. The crystal was irradiated in situ from an unpolarized Thorlabs Cold White LED (425−650 nm, SI Figure S1) for 2 h while continuously rotating the crystal in order to achieve the maximum uniformity of sample irradiation. Data were then recollected with an otherwise identical collection and integration procedure to the dark (GS only) data. The structures were solved by direct methods and refined by full-matrix least-squares methods on F^2 values of all data. Refinements were performed using SHELXL[14] with full details given in Supporting Information.

The ground-state structures of **1**−**3** were first determined. **1** and **2** were found to be isomorphous, crystallizing in the *Pmcn* space group, with the SO_2−Ru−**X** plane lying within the mirror plane; this mirror plane bisects two of the N−Ru−N angles. The S−Ru−N_{pyr} angle (178.8(1)° and 178.7(1)° for **1** and **2**, respectively) distorts an otherwise regular octahedral Ru coordination to a similar extent as other members of this family of complexes.[10−12] In contrast, **3** crystallizes in the non-centrosymmetric space group $P2_1$; nonetheless, its molecular conformation is identical to **1** and **2** within experimental error (SI Table S1). The only marked difference in molecular geometry between the three compounds is the Ru−N_{pyr} bond length, 2.115(2) Å for **1**, compared with larger values 2.131(3) and 2.123(4) Å, for **2** and **3**, respectively. This suggests that the pyridyl chloro-substitution withdraws electron density from the pyridyl nitrogen, weakening the Ru−N_{pyr} σ-bond, in turn strengthening the Ru−S σ-bond. This bond length trend correlates with the pK_a series for Lewis basicity of the ligands, as the more basic ligands donate more electron density into the Ru.

Following in situ irradiation, the photoexcited geometries of the three compounds were examined. After excitation, no change in space group was observed for any of the compounds. Considering **1** first, since this contains the unsubstituted pyridine ligand, the GS-only model was introduced; however this model was unstable due to the large amounts of electron density around the MS1 geometry (Figure 2a), so an MS1

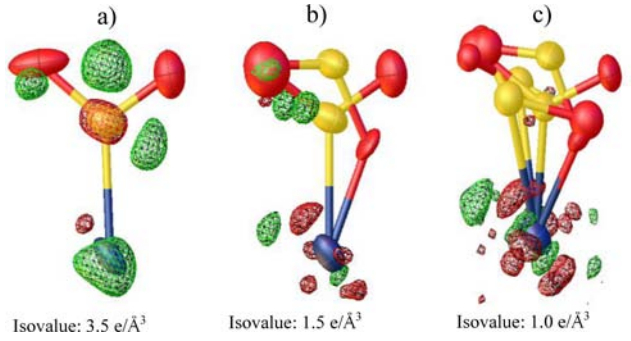

Figure 2. A 3D electron density map imaged using OLEX.[15] The green wire frame represents areas of positive electron density and the red represents areas of negative electron density. The isovalue is the electron density on the wireframe surface and the enclosed regions have an electron density of at least this isovalue. The yellow atoms represent sulfur, the red atoms represent oxygen, and the blue atoms represents ruthenium. (a) A large amount of positive electron density is shown around the MS1 geometry which was subsequently introduced. (b) A small amount of positive electron density is shown around the MS2 S and O_{free} geometry which again was subsequently introduced. (c) No positive electron density is shown near the SO_2 with only background noise present.

geometry was subsequently introduced. The resulting Fourier difference map (Figure 2b) again showed a small but distinct additional volume of unmodelled electron density, reminiscent of the S peak of the MS2 geometry, so this state was then introduced into the model. The final model afforded SO_2 occupational fractions of 44.5(7)% MS1, 42.4(9)% GS, and 13.2(9)% MS2, with an R1 of 0.0569 and wR2 of 0.1461 (Figure 2c). The resulting geometric positions of the MS1 O_{free} and one of the GS O atoms are only 0.20(4) Å apart, so appropriate partitioning of the electron density in this region is difficult. To achieve a stable model, these atoms were refined isotropically and their atomic displacement parameters were restrained to be the same within a standard deviation of 2%. Furthermore, owing to the small MS2 population, their SO_2 atoms were also refined isotropically.

The MS1 SO_2 photoisomer lies entirely within the crystallographic mirror plane, and its bond geometry is similar to that of the GS SO_2, with the S−O_{bound} bond, 1.50(2) Å, the S−O_{free} 1.47(2) Å, and an O−S−O angle 114.8(11)°. The *trans* O_{bound}−Ru−N_{pyr} angle of 165.2(5)° shows a significant distortion from linearity which is consistent with the values found by Bowes et al.[9] in the $[Ru(NH_3)_4SO_2H_2O]Tos_2$ complex. The O_{free} and S atoms of the MS2 state are disordered over two sites across the mirror plane; however, the

dx.doi.org/10.1021/ja303943q | J. Am. Chem. Soc. 2012, 134, 11860−11863

O_{bound} atom lies within the mirror plane and is therefore not disordered (Figure 2c). The bond lengths, S−O_{bound}, 1.61(9) Å, and S−O_{free}, 1.51(4) Å, and bond angle, 131(3)°, are similar to those of other previously known MS2 geometries.[8,10,11]

The presence of such a high level of photoconverted MS1 state at liquid nitrogen temperatures has allowed the decay kinetics to be readily examined for the first time. The temperature was initially raised from 100 to 120 K at 360 Kh^{-1} and five more full diffraction sets were collected successively over 12 h. The temperature was subsequently raised to 130 K at the same rate and nine full diffraction experiments were collected over 21 h, and the temperature was then raised to 140 K with six more full diffraction experiments collected repeatedly, yielding complete conversion from the MS1 geometry into the MS2 geometry (Chart 1). Initially the decay was modeled as traditional first- and second-order decay. However, this did not yield a good correlation with the data (SI Chart S1).

Chart 1. The Decay of the MS1 Geometry (Red) into the MS2 Geometry (Blue) at Different Temperatures[a]

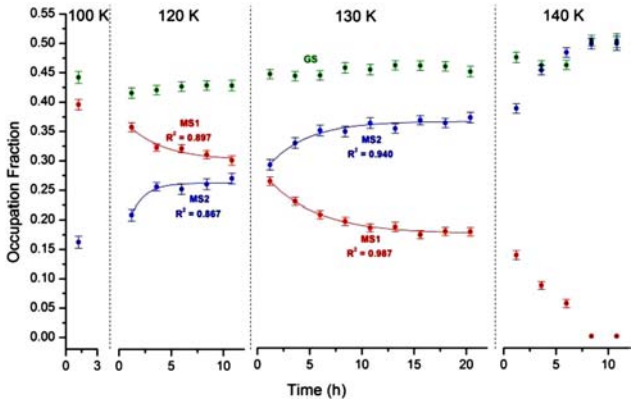

[a]Each data point represents a full diffraction experiment and its time is attributed to the midpoint of the relevant data collection. The time was re-started at each temperature change represented by the dotted lines. The GS occupational fraction is shown in green.

As such, different decay kinetics are proposed, with the MS1 decaying into a long lifetime at different temperatures. This was thus modeled as first-order decay with a non-zero asymptote:

$$f = A\ e^{-kt} + z$$

This produced a much better correlation with the data with a coefficient of determination, R^2, of 0.949 for 120 K data and R^2 of 0.990 for the 130 K data. From this, we can determine that at 120 K there is decay, over 7.0 h, from 39.6(7)% to a long-lived state of 30(1)% with a concomitant increase of the MS2 geometry and no discernible change in the GS occupation (Chart 1). At 130 K, there was further decay of the MS1 state reducing to a stable 17.4(3)% over 11.7 h, again decaying exclusively into the MS2 geometry. At 140 K, there was complete conversion from the MS1 geometry into the MS2 geometry (SI Figure S3a), but the decay was too rapid to harness sufficient data points with a laboratory diffractometer, so a decay rate could not be quantified. Although this model successfully fits the data, it is also possible that other, more complex, mixed-order kinetics are needed to model this behavior, such as explicitly resolving the spatial distribution of the excited states in a nonuniform excitation intensity pattern as described by Cambron et al.[16] Furthermore, the experiment was repeated to examine the 120 and 140 K kinetics for reproducibility which is challenging given the developing field of photocrystallography. Results are reproducible to occupancies within 5% of each other (SI Chart S2).

Considering the effects of chloro-substitution on the pyridine ring, **2** and **3** also showed photoisomerization around the SO_2 at 100 K. The photocrystallographic data were first modeled with only the GS SO_2 configuration. The resulting Fourier difference map revealed a small population of electron density for the MS2 state; so this state was introduced into the model affording an MS2 SO_2 occupation of 10.4(1)% and 18.2(7)% for **2** and **3**, respectively. For **2**, there was no evidence of the MS1 state (SI Figure S3b). However, for **3**, there was a small amount of electron density around the MS1 S, yet this electron density was too small to quantify (below ∼5%, SI Figure S3c). The MS2 SO_2 ligand state was disordered across the mirror plane for **2**, in a similar fashion to the MS2 state of **1**. However, no such disorder was found in the MS2 state of **3** presumably due to the lack of the mirror plane symmetry constraint with **3** belonging to the $P2_1$ space group, cf. **1** and **2**, which are in *Pmcn*. Owing to the small populations of the MS2 state, the MS2 SO_2 atoms were refined isotropically, but given the lack of overlap with the MS1 state in contrast to **1**, no restraints were needed for the atomic displacement parameters for **2** or **3**. The MS2 geometries of **2** and **3** are similar to that for **1**, with the exception of a longer S−O_{bound} bond of 1.82(5) Å for **2**.

The thermal stability of the MS2 state was then assessed for each compound **1**−**3**. The crystals were excited by the same LED light for 2 h at 150 K since this elevated temperature precludes any MS1 state formation; a combination of the GS and MS2 geometries was observed. The temperature was then raised from 150 to 200 K at 360 Kh^{-1} and the MS2 decay into the ground state was modeled via first-order kinetics, in common with the methods described by Kovalevsky et al.[10,11] Both **1** and **3** showed evidence of decay at 200 K, with a half-life of 15.6(9) and 12.6(4) h, respectively (Chart 2). On the other hand, **2** showed no decay over 10 h, after modeling 6 successive full diffraction data sets, suggesting long-term stability at 200 K. The temperature of **2** was subsequently raised to 220 K and the MS2 geometry decayed into the GS

Chart 2. MS2 Decay of Compounds 1−3[a]

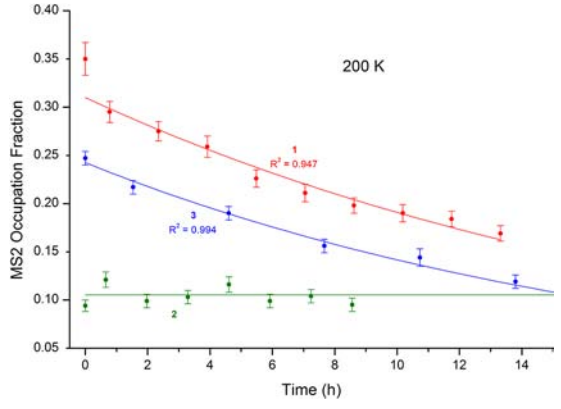

[a]Compounds **1** and **2** were collected with an orthorhombic strategy, with each data point collected over 93 min. **3** was collected with a monoclinic strategy with each data point collected over 187 min. Consequently, there are only half the number of points per unit time for **3** compared with that for **1** and **2**.

over 6 h. These results show that the MS2 geometry is most thermally stable at 200 K where 3-Cl-pyrdine is the *trans*-ligand, followed by pyridine as a *trans*-ligand, with 4-Cl-pyridine *trans*-ligand generating an MS2 geometry with the lowest thermal stability.

Since the only difference in chemical composition for **1**−**3** was the chloro-substitution on the pyridine group, the photoconversion and thermal stability of the MS2 state can be related to the *trans*-ligand. The pyridine ligand present in **1** is known to be a good σ-donor, reflected by its pK_a value (pK_a = 5.14),[17] and a poor π-acceptor. This σ-donating ability gives pyridine a high trans-influence in the ground state of **1**; as the σ-electrons enhance electron density around the Ru, the induced negative charge weakens the Ru−S σ-bond *trans* to the photolinkage isomer. This trans-influence creates a lower energy barrier for photoisomerization, allowing for a higher occupational fraction of photoconverted SO_2. The lower pK_a values for 3-Cl-pyridine and 4-Cl-pyridine (pK_a = 2.84 and 3.84, respectively)[17] indicate that they are weaker σ-donors, which in turn exhibit a weaker trans-influence affording a stronger Ru−S σ-bond in the GS. In the MS2 geometry, the S−O_{bound} π-electrons donate into the Ru σ-orbital, with the S−O_{bound} bond length increasing as the Ru−(S,O) bond strength increases. This is consistent with our experimental results with the S−O_{bound} bond lengths of 1.82(5) Å for **2**, 1.73(5) Å for **3**, and 1.60(8) Å for **1** following the same trend as the pK_a values for the *trans*-ligand. The other effect to take into account when examining the MS2 bonding mode is π-backbonding from the filled Ru dπ-orbital into the empty π^* orbital of the S and O atoms. The level of backbonding to the photolinkage ligand is inversely proportional to the π-acceptor ability of the *trans*-ligand, suggesting that the amount of backbonding increases from pyridine, 4-Cl-pyridine to 3-Cl-pyridine.

Examining the occupational fraction and the thermal stability of the MS2 geometry at 200 K for **1**−**3**, we observe trends consistent with the bonding mode described above. As the σ-donating strength of the *trans*-ligand increases, the occupational fraction of the MS2 state also increases in the order **2** < **3** < **1** as the energy barrier of the transition from the GS to the MS2 geometry is reduced. Furthermore, the presence of the MS1 state at 100 K in **1** and trace residues in **3** may be due to the wavelength required to excite the transition into this geometry being higher than 350 nm (the minimum wavelength of our light source). However, the transition might require a lower wavelength than this for **2**, due to the increased Ru−S bond strength. The thermal stability of the MS2 geometry decreases in the order **2** > **1** > **3** showing the competing effects between π-backbonding stabilizing **1** more than **3**; however, the long-term MS2 stability of **2** at 200 K shows that the stability is primarily controlled by the increased strength of the Ru−(S,O) σ-bond.

In summary, we have reported on three new *trans*-$[Ru(NH_3)_4(SO_2)X]Cl_2{\cdot}H_2O$ complexes to investigate the stability of the MS1 and MS2 photoexcited states. We have found the existence of the MS1 state for compound **1** with a very high 44.5(7)% occupation at 100 K and shown that this state decays via first-order kinetics with a non-zero asymptote with a long lifetime at 120 and 130 K before complete decay into the MS2 geometry at 140 K. Furthermore, we have afforded the decay kinetics across a group of *trans*-ligands based on a pyridyl derivative and found that the MS2 geometry is primarily stabilized by the increased strength of the Ru−(S,O) σ-bond; however, π-backbonding does also have an effect. This knowledge establishes a design protocol for future members of this family allowing one to intelligently control their photoconversion levels and thermal stability.

■ ASSOCIATED CONTENT

Supporting Information

Experimental procedures, refinement details, repeatability of decay kinetics, Hirshfeld surface analysis of MS2 induced strain, Fourier difference maps and selected crystallographic information. This material is available free of charge via the Internet at http://pubs.acs.org.

■ AUTHOR INFORMATION

Corresponding Author

jmc61@cam.ac.uk

Notes

The authors declare no competing financial interest.

■ ACKNOWLEDGMENTS

S.O.S. thanks the Cambridge Commonwealth Trust for a graduate student scholarship. J.M.C. thanks the Royal Society for a University Research Fellowship, the University of New Brunswick for the UNB Vice-Chancellor's Research Chair and NSERC for the Discovery Grant, 355708 (for P.G.W.).

■ REFERENCES

(1) Goulkov, M.; Schaniel, D.; Woike, T. *J. Opt. Soc. Am. B* **2010**, *27*, 927.
(2) Imlau, M.; Fally, M.; Weisemoeller, T.; Schaniel, D.; Herth, P.; Woike, T. *Phys Rev B* **2006**, *73*, 205113.
(3) Imlau, M.; Woike, T.; Schaniel, D.; Schefer, J.; Fally, M.; Rupp, R. A. *Opt. Lett.* **2002**, *27*, 2185.
(4) Cole, J. M. *Chem. Soc. Rev.* **2004**, *33*, 501.
(5) Cole, J. M. *Z. Kristallogr.* **2008**, *223*, 363.
(6) Cole, J. M. *Acta Crystallogr., A* **2008**, *64*, 259.
(7) Coppens, P. *Angew. Chem., Int. Ed.* **2009**, *48*, 4280.
(8) Phillips, A. E.; Cole, J. M.; d'Almeida, T.; Low, K. S. *Phys. Rev. B* **2010**, *82*, 155118.
(9) Bowes, K. F.; Cole, J. M.; Husheer, S. L. G.; Raithby, P. R.; Savarese, T. L.; Sparkes, H. A.; Teat, S. J.; Warren, J. E. *Chem. Comm* **2006**, *23*, 2448.
(10) Kovalevsky, A. Y.; Bagley, K. A.; Cole, J. M.; Coppens, P. *Inorg. Chem.* **2003**, *42*, 140.
(11) Kovalevsky, A. Y.; Bagley, K. A.; Coppens, P. *J. Am. Chem. Soc.* **2002**, *124*, 9241.
(12) Phillips, A. E.; Cole, J. M.; d'Almeida, T.; Low, K. S. *Inorg. Chem.* **2012**, *51*, 1204.
(13) Chatt, J.; Duncanson, L. A. *J. Chem. Soc.* **1953**, *65*, 2929.
(14) Sheldrick, G. *Acta. Crystallogr., A* **2008**, *64*, 112.
(15) Dolomanov, O. V.; Blake, A. J.; Champness, N. R.; Schroder, M. *J. Appl. Crystallogr.* **2003**, *36*, 1283.
(16) Cambron, R. T.; Zhu, X. R.; Harris, J. M. *J. Phys. Chem.* **1994**, *35*, 8726.
(17) Uruska, I.; Szpakowska, M. *Fluid Phase Equilib.* **1991**, *62*, 141.